Surgical Motion Adaptive Robotic Technology (S.M.A.R.T): Taking the Motion out of Physiological Motion

Anshul Thakral, Jeffrey Wallace, Damian Tomlin, Nikesh Seth, and Nitish V. Thakor

Department of Biomedical Engineering, Engineering Research Center for Computer Integrated Surgical Systems and Technology
The Johns Hopkins School of Medicine, Baltimore, Maryland 21205 USA
nthakor@bme.jhu.edu

Abstract. In precision computer and robotic assisted minimally invasive surgical procedures, such as retinal microsurgery or cardiac bypass surgery, physiological motion can hamper the surgeon's ability to effectively visualize and approach the target site. Current day stabilizers used for minimally invasive cardiac surgery often stretch or pull at the tissue, causing subsequent tissue damage. In this study, we investigated novel means of modeling Z-axis physiological motion and demonstrate how these models could be used to compensate for this motion in order to provide a more stable surgical field. The Z-axis motion compensation is achieved by using a fiber-optic laser sensor to obtain precise displacement measurements. Using a weighted time series modeling technique, modeling of rodent chest wall motion and heart wall motion was accomplished. Our computational methods for modeling physiological motion open the door for applications using high speed, high precision actuators to filter motion out and provide for a stable surgical field.

1. Introduction

In order to perform accurate surgical procedures, surgeons need a well-exposed and immobilized target site. Creating a well-exposed bloodless surgical field is not as difficult as creating a motionless surgical field. Often moving organs, such as the beating heart, present an added challenge for surgeons to overcome the physiological motion. In cardiac surgery, the heart is traditionally stopped using cardiopulmonary bypass (CPB) to stop this motion. The use of CPB, however, causes many damaging effects to the patient's blood, and often leads to higher costs and recovery times [1]. Even with current day minimally invasive procedures, which are aimed to reduce blood trauma and post-operative complications [2], physiological motion can severely impair the ability of surgeon to effectively operate. During procedures such as minimally invasive direct coronary artery bypass (MIDCAB) surgery, or surgery on a beating heart, sutures placed by a surgeon often rip or tear due to the physiological motion of the heart, which can exceed 1.3 cm of outward expansion [3]. Several methods have been applied to this problem of dealing with motion in the surgical field

W. Niessen and M. Viergever (Eds.): MICCAI 2001, LNCS 2208, pp. 317-325, 2001.

in an attempt to eliminate the hindrances and try to increase the performance of the surgeon.

Current day commercial solutions to the problem of physiological motion involve the use of tissue stabilizers. These stabilizers either use pressure [4] or suction [5] on the tissue to achieve a psuedo-motionless environment. The stabilizers that work by means of pressure only work on grafting to the exterior surfaces of the heart. Suction methods often damage the myocardial tissue, even when used for short periods of time [6]. The use of motion platforms that moves the surgeon's hands in synchrony with either a set of oscillatory motors and pacing the heart [3], or optical and mechanical sensors with feedback [6] have been published. These methodologies have shown that surgeons can perform delicate tasks, such as anastomosis on a moving surface, but include hindrances such as being cumbersome, or invasive.

The ideal solution for motion compensation during surgical procedures would be to provide motion-tracking capabilities using algorithms to filter out the motion, while using high precision robotic systems through minimally invasive ports.

We propose a solution involving the use of novel adaptive motion tracking algorithms to compensate for periodic and quasi-periodic physiological motions. Adaptive filtering, which has been around since the 1950's to study periodic signals [7], allows modeling of the physiological information in an updateable model. By obtaining the tissue surface displacement measurements, we are able to create adaptive models of the both chest wall and heart wall motion from a surgically prepared rodent. In this paper, we compare several different adaptive algorithms and are able to determine the characteristics and uses of the algorithms for the motion compensation problem. Although it is beyond the scope of our experiments, given these adaptive models, a high speed robotic actuator would be able to compensated for the motion by using the models as a motion predictor, and keeping the tissue surface approximately still from the perspective of the tool on the robotic actuator.

2. Methods

A. Rat Chest Wall and Heart Wall Model

In order to simulate physiological motion for our algorithms, rodent chest wall and heart wall motion was exposed during our surgical procedure. To provide controlled breathing patterns, the test subjects (8 Wistar rats, 300 ± 25g) underwent anesthesia and were placed on ventilator systems for intubation. The subjects were anesthetized with 4% halothane and 50:50% nitrous oxide:oxygen, in a small place chamber. Once unconsciousness, the rats was placed in a supine position and two needle electrodes were inserted in the arm and leg of the rat to provide an electrocardiogram (ECG) for reference purposes.

For chest wall motion measurements, the chest of the rat was shaved to provide a smooth and clean surface for measurement. The recording instrumentation was placed next to the rodent, with the extension arm and displacement sensor placed directly 1cm above the chest. Measurements were taken for 2 minutes intervals and repeated 3 times before the sensor was moved to a different portion of the chest. To

keep the data synchronized with the ECG data, it was recorded via the same A/D converter and Pentium level computer.

After the chest wall measurements were concluded, the rats were subjected to partial thoracothomy on the left side, about halfway down the ribcage, to provide access to the heart. After this was completed, the heart could be seen and the fiber optic probe attached to the instrumentation could be carefully inserted to within 1cm of the heart wall. Again, measurements were taken for 2 minute intervals and repeated 3 times before recording from a different angle.

B. Instrumentation Setup

For our experiments, we used a M-511 series linear stage micropositioner from Physik Instruments (Waldbronn, Germany), which provides 0.1 micrometer minimum incremental motion and a one micrometer full travel accuracy, as our micropositioner and the basis for our microsurgical robotic arm for recording. This microsurgical robotic arm consists of the micropositioner, a base with an x-z brace that allows for a z-axis setup, an extension arm, and a mount for the displacement sensor (Figure 1). The arm was extended 18 inches out from the faceplate of the M-511, and the fiber optic probe was held in place to record the displacement.

For the recording of biological tissue displacement, we used a D169 fiber optic displacement sensor from Philtec, Inc. (Annapolis, MD USA), which has a linear measurement range of 0.8 to 21.6 mm, with an operating resolution of 3.18μm. The output of the sensor provided a 0 to 5 V analog signal that was directly proportional to the distance being measured. The output was calibrated with a simple y = m(x) + b equation, using several known distances and a simple best fit algorithm. The analog signal from the fiber optic sensor was converted into a digital signal with the use of a Daytronic 2160 Digital Panel Meter (Daytronic Inc, Dayton, Ohio). The digital signal was then transferred to a computer for recording through a RS232 serial port. The acquisition software was written on a Windows 9X platform using Visual C++ (Microsoft, Redmond, WA.) and the analysis was performed in MATLAB (Mathworks, Natick, MA).

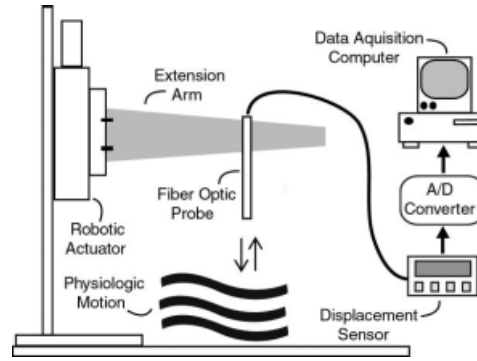

Figure 1: The data acquisition setup for our experiments. The fiber optic probe used to record physiologic motion, was positioned and calibrated with the use of the robotic actuator depicted above.

C. Adaptive Algorithms

Adaptive filters and algorithms have been around since the late 1950's as a type of self-learning filter [7]. These filters have a set of predetermined initial conditions, and are able to learn input statistics progressively, and adjust its coefficients in order

to minimize error criterion. In static environment, these filters converge to optimum "Wiener" filters after successive iterations [8]. Windrow and Hoff's least mean square (LMS) algorithm is one of the most widely used adaptive filters [9].

Certain physiological motions, such as heart wall and chest wall motion in our experiments, can be modeled as periodic signals that repeat consistently with a set reference, such as heart beat or respiratory rate. A discrete Fourier series model (FSM) can be used to represent the periodic components of certain physiological motions [10]. In the FSM equation (Equation 1), w_o is the fundamental frequency, M is the model order required to cover the entire signal bandwidth, and $\{a_m, b_m\}$ are the m^{th} Fourier coefficients of the periodic signal. The assumption here is that physiological motion can be broken down into discrete sinusoidal components and then can be recomposed by summing weighted versions of the sinusoids.

$$s(k) = \sum_{m=1}^{M} a_m \sin(m\omega_0 k) + b_m \cos(m\omega_0 k) \tag{1}$$

In the Fourier Linear Combiner (FLC) algorithm, the reference signal is comprised of different harmonics of the defined fundamental frequency (Equation 2). The reference signal is used to create a model of the input signal. X_k consists of a sine and cosine term for each of m harmonics, and depending on the model order of our input signal, this can be truncated to only a few harmonics without significant distortion.

$$\underline{X}(m,k) = [\sin(m\omega_0 k); \cos(m\omega_0 k)]^T \qquad ; m = 1,..,M \tag{2}$$

The weight vector, Wk, is used to create a filtered output that models the observed signal, and thus compensating for the periodic physiological motion (Equation 3). The modeled signal is the weighted sum of the input sinusoids, thus the filtered output is found by taking the inner product of the input vector and the weight vector, which is the instantaneous estimate of the Fourier coefficients. Weights are updated using mean squared error method between the modeled and reference signal. To reduce the computational load, the model order, M, is chosen so that the truncated series represents more than 95% of the signal power.

$$\underline{W}(k) = [w_1, w_2, ..., w_{2M-1}, w_{2M}]^T \tag{3}$$

The FLC algorithm has been shown to be computationally inexpensive as compared to other adaptive filter [11], have inherently zero phase [12], and has an infinite null [13]. FLC can be viewed as an adaptive notch filter at w_0, with width equal to the adaptive gain parameter, m [13]. The time constant of the filter is a representation of its memory, or the number of sample points it "remembers" in order to compute the estimates.

The FLC, however, operates at a fixed frequency, and cannot compensate for changes in both frequency and amplitude. The Weighted Frequency Fourier Linear Combiner (WFLC) forms a dynamic truncated Fourier series model of the desired input signal, and adapts to frequency of the model as well as the Fourier coefficients [14]. The fundamental frequency in the FLC algorithm, w_0, is replaced by a set of adaptive frequency weights, w_{0k}. Thus the modeled signal is no longer represented by inner product of the weights and reference signal, but by Equation 4. Using the simplified approach underlying the LMS algorithm, an adaptive recursion for w_{0k} can be created in the same amount of time using Equation 5. An adaptive gain parameter, μ_0, has been added to the frequency weights in order to tune the filter. Equation 5 is

used to update the frequency weights, and the rest of the algorithm proceeds similar to the FLC algorithm. It has been published that for small enough m_0, w_{0k} actually converges to the frequency of the sinusoidal input signal [15]

$$\hat{d}(k) = \sum_{r=1}^{M} [w_{rk} \sin(rw_{0k}k) + w_{r+Mk} \cos(rw_{0k}k)] \quad (4)$$

$$w_{0_{k+1}} = w_{0_k} - 2\mu\varepsilon_k \frac{\partial \varepsilon_k}{\partial w_{0_k}} \quad (5)$$

In cases like ours, it is important to have a fast tracking algorithm with minimal misadjustment, to avoid the loss of data. To accomplish this, we added a variable step size LMS algorithm [16] to our adaptive algorithm to create an Adaptive Fourier Linear Combiner (AFLC). The gain parameter, μ in Equation 5, is now represented by a dynamic gain parameter, μ_k as in Equation 6 and is adjusted by square of the prediction error. Since only one more update in needed is each step of the algorithm, the AFLC algorithm is only minimally more complex than the FLC algorithm, but has adaption capabilities.

$$\underline{W}_{k+1} = \underline{W}_k + 2\mu_k e_k \underline{X}_k \quad (6)$$

For applications, involving complex signals, neither the AFLC Algorithm nor WFLC algorithm alone can compensate for such a signal. To solve this, we employed a technique that uses both the AFLC algorithm and WFLC, in order to model the signal, named the Tiered Fourier Linear Combiner (TFLC) algorithm. In this algorithm, the recorded signal passes through an AFLC routine, which results in a modeled chest wall signal and an error component. This error component is then passed through a WFLC routine to result in a modeled heart wall signal. The two modeled signals are then simply combined to produce the modeled version of the original complex signal.

3. Results and Discussion

A. Characterization of the FLC and WFLC Algorithm for Rat Heart Wall Data

A 30 second segment of the rat heart wall data is run through the FLC algorithm. Trials were run for model order (M) set at 2nd, 3rd, and 4th order. For each value of M, the data was iterated through a series of μ values, which are the adaptive gain factor, and the resulting percent error was recorded. This data is summarized in Figure 2, where we can see that as expected, increasing the μ value helps reduce the error signal. Also we see that at higher μ values, increasing the model order helps lower the percent error; however at lower μ values the difference within model orders is not as significant.

To better understand the advantages of the WFLC over the FLC, the data used in Figure 2 were analyzed using the WFLC algorithm, where the recorded ECG signal is set to the reference signal. The data are summarized in Figure 3, where we can see a drop in percent error with an increase in μ values. With the WFLC algorithm, however, the model order M does not have as much of an effect. The WFLC algorithm's performance is more independent of model order then the AFLC

algorithm. Also, we see that with the WFLC algorithm we are able to achieve a lower percent error than with the FLC algorithm, at all model orders.

B. WFLC and TFLC Algorithms Performance Under Varying Signal to Noise Ratios

The efficiency of the AFLC algorithm is dependent on the signal to noise (SNR) ratio of the input signal. In order to determine the performance of the algorithms, we simulated signals with varying SNR. To generate signals with varying SNR, we used recorded pure chest wall (left side of the rat's chest) as the signal, and recorded data of the rat's heart wall to represent the noise on the heart wall. By varying the amplification of the 'noise', several different signals of different SNR were created. Figure 4 shows the performance of the WFLC algorithm compared to the TFLC for different SNR input signals. For the higher SNR signal (Figure 4a), the TFLC had an mean error of 10.3%, while the WFLC resulted in a 12.3% error. For the lower SNR case (Figure 4b), the TFLC resulted in a 23.1% error, while the WFLC resulted in a 34.1% error. In both cases, the TFLC outperforms the other showing its resilience within a noisy environment.

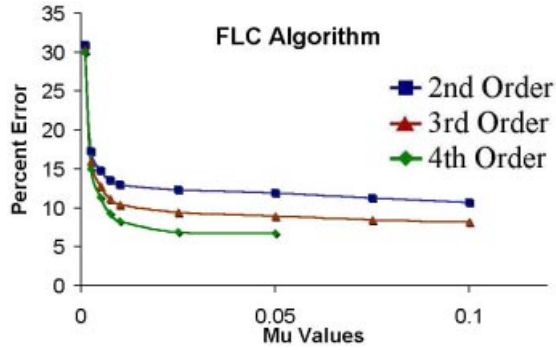

Figure 2: By increasing the value of the adaptation variable μ, the performance of the FLC algorithm was tested for three different M orders (2nd, 3rd, and 4th)

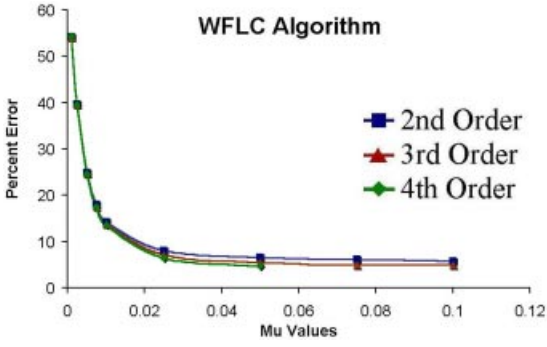

Figure 3: Performance analysis of the WFLC algorithm for different values of μ and different M orders (2nd, 3rd, and 4th). Unlike the FLC algorithm, the WFLC's performance is not as dependent on the order of M.

C. Modeling of Complex Signal with the TFLC Algorithm

We used chest wall recordings from over the heart as a complex signal to be modeled by the TFLC algorithm. The biological motion recorded by the fiber optic sensor is considered complex because it contains both motion from the respiration and motion from the heart wall underneath the surface of the skin. By taking the FFT of the recorded data from the complex motion, two strong spikes were seen in the spectral plot. The stronger of the two spikes is seen at 0.6 Hz and the second non-harmonic spike was at 5.5 Hz. From this observation, we can see both the chest wall as well as

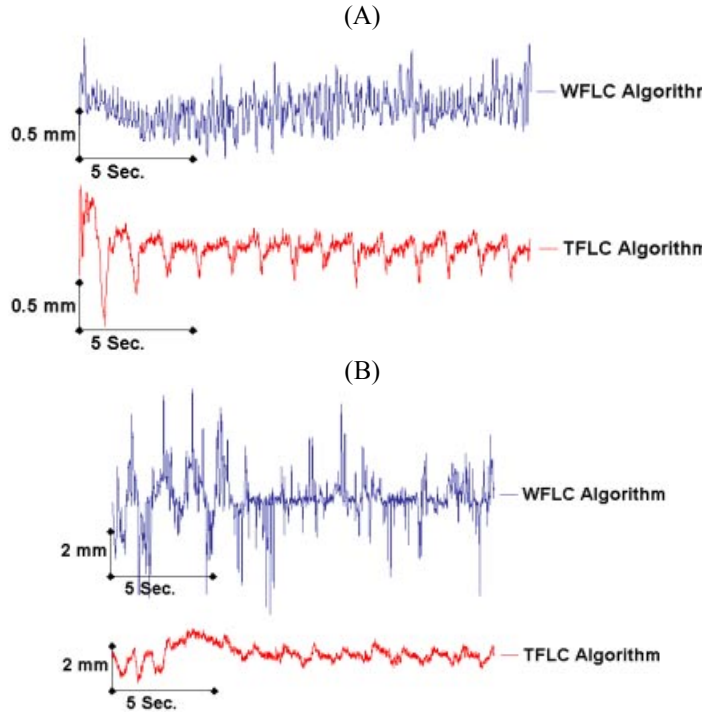

Figure 4: The comparison of the AFLC and TLC algorithms under different signal to noise ratios (SNR). For the high SNR case (A) where the SNR is –4 dB, the TFLC has a mean error of 10.3% while the WFLC has a mean error of 12.3%. For the low SNR case (B), where the SNR is –9 dB, the TFLC has a mean error of 23.1% and the WFLC has a mean error of 34.1%. In both cases, the TFLC outperforms the WFLC, even in noisy environments (low SNR).

the heart wall motion in the signal. The 0.6 Hz signal corresponds to the chest wall (respiration was set at 45 breaths per minute) and the 5.5 Hz component corresponds to the heart wall motion, (5.5 Hz was the primary frequency in the recorded ECG signal). Modeling the signal using the TFLC algorithm resulted in a signal that had a mean error of only 10%. Figure 5 show the modeled signal plotted with the recorded signal that was used. As demonstrated with this model, even with a complex biological signal, the TFLC can model the signal to a high accuracy.

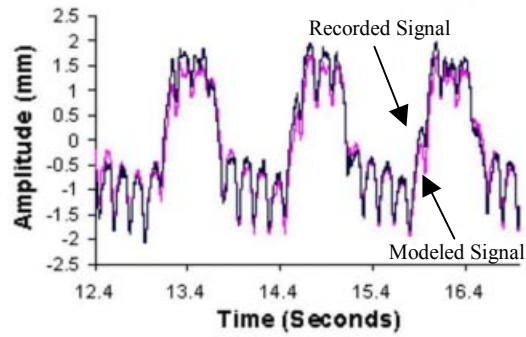

Figure 5: The recorded complex signal of the rat chest wall and heart wall displayed with the resulting modeling signal. The model was generated with the TFLC algorithm.

4. Conclusions

Complex physiological motion can severely limit a surgeon's ability to perform accurate and efficient procedures. In many cases, as in beating heart surgery, the motion limits surgery only to the simplest of procedures. If this motion can be filtered out of the surgical field without being invasive, the possibilities of minimally invasive surgery will increase dramatically.

This paper demonstrates the functionality and performance of adaptive algorithms and their ability to model complex biological signals. Future implementation of these adaptive algorithms into high-speed robotic actuators will allow motion to be both adaptively modeled as well as use this model as a next step predictor in an attempt to move the tool time in synchrony with the tissue motion. Therefore, from the point of view of the actuator's tool tip, the field will be approximately motionless, as the motion has been filtered out. With the use of adaptive algorithms, motion within a surgical field can be greatly reduced or even eliminated, making procedures that were impossible or incredible difficult, something that is within reach for an average surgeon.

References

1. Ko, W. *Advances in Cardiovascular Surgery - Minimally Invasive Cardiac Surgery*. in *1997 CAMS Semiannual Scientific meeting*. 1997. New York.
2. Matsuda, H., *et al.*, *Minimally Invasive Cardiac Surgery: Current Status and Perpective.* Artificial Organs, 1998. 22(9): p. 759-64.
3. Mayer, P.W., *Relative Motion Cancelling*, in *Patent No. 5871017*. 1999: US.
4. Rousou, J.A., *et al.*, *Fenestrated felt facilitates anastomotic stability and safety in & "off-pump" coronary bypass.* Ann Thorac Surg, 1999. 68(1): p. 272-3.
5. Jansen, E.W.L., *et al.*, *Coronary Artery Bypass Grafting Without Cardiopulmonary Bypass Using the Octopus Method: Results in the First One Hundred Patients.* The Journal of Thoracic and Cardiovascular Surgery, 1998. 116(1): p. 60-67.
6. Trejos, A.L., *et al. On the Feasibility of a Moving Support for Surgery on the Beating Heart*. in *Medical Image Computing and Computer-Assisted Intervention - MICCAI'99: Second International Conference*. 1999. Cambridge, UK.
7. Widrow, B. and S.D. Stearns, *Adaptive signal processing*. Prentice-Hall signal processing series. 1985, Englewood Cliffs: Prentice-Hall. xviii, 474.
8. Walter, D.O., *A posteriori Wiener Filtering of average evoked responses.* Electroencephalogr Clin Neurophysiol, 1968. :Suppl(27): p. 61+.
9. Widrow, B. and J. M.E. Hoff. *Adaptive switching circuites*. in *IRE WESCON Conv. Rec.* 1960.
10. Metz, S., *An Intraoperative Monitoring System for the analysis of Evoked Potentials*, in *Biomedical Engineering*. 1999, Johns Hopkins University: Baltimore. p. 159.
11. Vaz, C.A. and N.V. Thakor, *Adaptive Fourier estimation of time-varying evoked potentials.* IEEE Trans Biomed Eng, 1989. 36(4): p. 448-55.
12. Riviere, C.N., *Adaptive suppression of tremor for improved human-machine control.*, in *Biomedical Engineering*. 1995, Johns Hopkins Univesity: Baltimore, Md.
13. Vaz, C., X. Kong, and N.V. Thakor, *An adaptive estimation of periodic signals using a Fourier linear combiner.* IEEE Transactions in Signal Processing, 1994. 42: p. 1-10.
14. Riviere, C.N., R.S. Rader, and N.V. Thakor, *Adaptive canceling of physiological tremor for improved precision in microsurgery.* IEEE Trans Biomed Eng, 1998. 45(7): p. 839-46.

15. Gresty, M. and D. Buckwell, *Spectral analysis of tremor: understanding the results.* J Neurol Neurosurg Psychiatry, 1990. 53(11): p. 976-81.
16. Kwong, R. and E. Johnston, *A Variable Step Size LMS Algorithm.* IEEE Transactions in Signal Processing, 1992. 40(7): p. 1633-1642.